Fabrication of Lightweight Microcellular Polyimide Foams with Three-Dimensional Shape by CO2 Foaming and Compression Molding

ARTICLE *in* INDUSTRIAL & ENGINEERING CHEMISTRY RESEARCH · SEPTEMBER 2012

Impact Factor: 2.59 · DOI: 10.1021/ie3017658

4 AUTHORS, INCLUDING:

Wentao Zhai
Chinese Academy of Sciences
62 PUBLICATIONS **978** CITATIONS
SEE PROFILE

Wen-Ge Zheng
Chinese Academy of Sciences
50 PUBLICATIONS **1,218** CITATIONS
SEE PROFILE

I&EC research
Industrial & Engineering Chemistry Research

Article

pubs.acs.org/IECR

Fabrication of Lightweight Microcellular Polyimide Foams with Three-Dimensional Shape by CO_2 Foaming and Compression Molding

Wentao Zhai,* Weiwei Feng, Jianqiang Ling, and Wenge Zheng

Ningbo Key Lab of Polymer Materials, Ningbo Institute of Material Technology and Engineering, Chinese Academy of Sciences, Ningbo, Zhejiang Province, 315201, China

ABSTRACT: Microcellular structure endows polymeric foams with the improved mechanical properties, but the preparation of lightweight microcellular polyimide (PI) foams with a large size is challenging and inefficient, because of low gas solubility, high stiffness, and an extremely long saturation time. In this study, PI foam was prepared by solid-state microcellular foaming technology with the compressed CO_2 as a physical blowing agent and tetrahydrofuran as coblowing agent. The presence of coblowing agent was verified to increase the gas sorption of PI, causing a dramatic increase in the expansion ratio of microcellular PI beads from 2.9 to 15.7. Using a novel compression molding process, the prepared PI foams were molded into the 3-D shaped products. Before the molding, the foamed PI beads were coated by poly(ether imide) (PEI)/chloroform solution. The contact angle tests indicated that PEI/chloroform could infiltrate well PI foams' surface, which facilitated the formation of strong interbead bonding between bead foams. The thickness of the coated PEI layer and the interbead bonding regions were the important parameters to adjust the bending and compression properties of the molded PI foam (MPI) product. The experimental results indicated that the bending strength and compression strength (at 10% strain) of MPI sample with density of 137.7 kg/m^3 were 1.27 and 1.59 MPa, respectively.

INTRODUCTION

Over the past decades considerable efforts have been put forth to fabricate lightweight polyimide (PI) foams, considering their superior heat-resistance, flame retardancy, and less smoke generation, which make them widely used in many advanced applications, such as aerospace, submarine, special ships, and high-speed trains.[1−4] However, most PI foams have cell sizes in the range of millimeters. The mechanical properties of these foams are usually much weaker than those of the solid polymers. Glass fiber-plastic honeycombs and aramid paper honeycombs sandwich structures could offer very unusual properties to military aircraft, such as low observability, remarkable toughness, and damage-resistance, but very high cost generally restricts their use. Consequently, it is very important to develop new high-performance lightweight materials with good mechanical properties at relatively lower cost.

Solid-state microcellular foaming technology has been suggested by researchers as a way to fabricate microcellular PI and other high-performance polymers foams to improve the mechanical properties. During the process, polymer resins are saturated by a physical blowing agent such as CO_2 and N_2 at high pressure and low temperature, and then foam at high temperature.[5−16] Krause et al. systematically investigated the microcellular foaming behaviors of poly(ether sulfone) (PES),[5−7] polysulfone (PSU),[6] and poly(ether imide) (PEI)[7] using CO_2. In those studies, the polymeric foams with microcellular structure and nanocellular structure could be obtained by adjusting the foaming parameters. In other studies of PEI foaming,[11,12] Miller et al. found that the presence of microcellular structure with cells in the range of 10 μm increased the strength-to-weight ratio of PEI obviously. Furthermore, they demonstrated that the nanocellular structures with cells in 50−100 nm range resulted in a further improvement in the modulus of toughness by up to 350% and in the impact energies by up to 600% compared to microcellular foams.[12] The fabrication of microcellular and nanocellular structure was an effective approach to improve the mechanical properties of PI foams. However, it is challenging to prepare microcellular PI foams with the expansion ratio higher than 10 times and densities comparable to the conventional PI foams.

Another challenge for solid-state microcellular foaming technology is its time-consuming nature, especially for the thick samples. As reported by Miller et al., the saturation time of PEI sheets with a thickness of 1.5 mm using CO_2 was about 500 h at 1 MPa and 350 h at 5 MPa,[10] while the saturation time for the PEI membrane with thickness of 0.075 mm required only 2 h at 1 and 4.6 MPa.[5] The extremely long saturation time is unfavorable to the fabrication of microcellular PI foam with a large-size and thus restricts the commercial application of microcellular foaming technology.

In this study, a novel microcellular PI bead foam preparation and molding technology is addressed to fabricate lightweight PI foam product with a large size. PI pellets were pelletized into small beads with diameter of 1.2−1.4 mm and aspect ratios of 1.5−2.0. Compressed CO_2 was used as a physical blowing agent, and an organic coblowing agent was selected to shorten the saturation time and to increase the expansion ratio of

Received: July 4, 2012
Revised: August 16, 2012
Accepted: September 4, 2012
Published: September 4, 2012

dx.doi.org/10.1021/ie3017658 | *Ind. Eng. Chem. Res.* 2012, 51, 12827−12834

microcellular PI foam. The prepared microcellular PI beads were coated with PEI solution, and then molded by compression molding. The infiltration character of PEI solution on PI foams' surface was investigated by scanning electron microscope (SEM) observation and contact angle analysis. The thickness of the coated PEI layer and the interbead bonding regions were adjusted as important parameters to investigate their effects on the interbead bonding and then the compression properties of the molded PI foam (MPI) products. The present study developed a novel and simple approach to fabricate the lightweight microcellular PI foam product with large size and three-dimensional shape. The well-defined properties potentially ensure microcellular PI foams to be used in many advanced applications.

EXPERIMENTAL SECTION

Materials and Preparation of the Solid Pellets. Thermoplastic polyimide resins (YZPI-JL10 and ULTEM-1010) were supplied by Nanjing Yuezi Chemical Ltd. and SABIC, and were coded as PI and PEI, respectively. According to the suppliers, the PI and PEI resins are amorphous with glass transition temperature (T_g) of 265 and 217 °C, respectively. The chemical structure of PI is shown in Scheme 1. CO_2 with a purity of 99.9% obtained from Ningbo Wanli Gas Corporation was used as the physical blowing agent. Tetrahydrofuran (THF) of reagent grade was obtained from Sinopharm Chemical Reagent Co., Ltd. and selected as the coblowing agent for polymeric foaming. Chloroform of reagent grade was obtained from Sinopharm Chemical Reagent Co., Ltd. and used as received. The PI pellets were dried in the oven for 12 h at 150 °C before use. PI beads with diameter of 1.2−1.4 mm and aspect ratio of 2.0 were prepared by extrusion pelletization at temperatures of 360−370 °C.

Scheme 1. Chemical Structure of PI

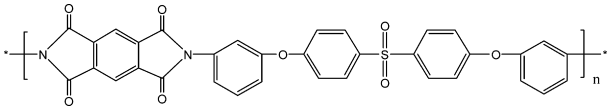

Autoclave Foaming. The PI beads (200 g) together with THF (50 mL) were placed in a high-pressure vessel (1 L) with the treatment temperature of 80 °C. Then the vessel was flushed with low-pressure CO_2 for about 3 min and then pressurized to 5 MPa. After the treatment of PI beads for one week, the samples were removed from the vessel after a rapid quench of pressure (2 MPa/s) and were transferred to a baking oven with a temperature of 270 °C. The foamed samples were removed out of oven after 60 s of foaming. In the case of PI foaming using CO_2, the saturation time at 5 MPa and 80 °C was three weeks, and the same conditions with the former were carried out during the foaming.

Compression Molding. PEI pellets were dissolved into chloroform at 80 °C with the aid of vigorous stirring. The foamed PI beads were put into the PEI/chloroform solution and were mixed using a glass rod. The PEI-coated PI foams were rapidly transferred into a mold cavity that was connected with hot plates. The fixed temperatures of the hot plates were 200 °C. After the filling, the bead foams were compressed with pressures of 2−8 MPa until the organic solvent was evaporated completely. The PEI layers solidified and then generated strong interbead bonding among bead foams.

Characterizations. The densities of PI bead (ρ) and foamed PI beads (ρ_f) were measured via the water displacement method in accord with ASTM D792, and the apparent density of the MPI samples (ρ_{mf}) was measured based on ASTM 1895. ϕ is the volume expansion ratio of the polymer foam, which can be calculated using eq 1 as follows:

$$\phi = \frac{\rho}{\rho_f} \tag{1}$$

The morphology of the foamed samples was observed with a Hitachi TM-1000 scanning electron microscope (SEM). The samples were freeze-fractured in liquid nitrogen and sputter-coated with gold. Both cell size and cell density were determined from the SEM micrographs. The cell diameter was the average of sizes of at least 100 cells on the SEM micrographs. The cell density (N_0), the number of cells per cubic centimeter of solid polymer, was determined using eq 2 as follows:

$$N_0 = \left[\frac{nM^2}{A}\right]^{3/2}\phi \tag{2}$$

where n is the number of cells in the SEM micrograph, M is the magnification factor, and A is the area of the micrograph (in cm^2).

The contact angle measurement was conducted on a contact angle system (OCA20) to study the affinity of PEI layer and PI foam. Before the measurement, the surface of PI foams was cleaned by anhydrous ethanol and then the foams were transferred to vacuum drying oven with the setting temperature of 100 °C for 12 h to remove the residual ethanol. The PEI/chloroform solution droplet was placed onto a flat homogeneous PI foam surface and simultaneously the contact angle of the droplet with the surface was measured. For each sample, 5 random locations were tested, and the average value is reported.

Rectangular and circular specimens were prepared from the MPI samples for the bending and compression tests. The typical dimensions of the specimens for bending were as follows, thickness = 20 mm, width = 25 mm, and length = 120 mm, and the dimensions for the compression tests were as follows, diameter = 100 mm and thickness = 20 mm. Bending strength testing was carried out according to ASTM C393-00 on an Instron testing machine at a crosshead speed of 10 mm/min, and compression strength testing was carried out based on ASTM365-03 with a crosshead speed of 2 mm/min. At least five specimens were tested under each condition, and the average value was used in this paper.

RESULTS AND DISCUSSION

Preparation of Microcellular PI Foams with High Foam Expansion. As shown in Table 1, the microcellular foams of high-performance polymers, such as PEI[6,11,12,16] and PES[15,16] foams exhibit low expansion ratio, which restrains their usage in aerospace and special ships. To increase the foam expansion, in this study, an organic solvent, THF, was used as coblowing agent together with compressed CO_2. Figure 1 shows the optical micrograph of PI beads and the foamed PI foams. It is seen from Figure 1c that the prepared yellow PI beads possess nice surface with the increased volume. Specifically, the diameter of PI bead increased from 1.2 to 1.4 mm up to 4.0−4.5 mm, which suggests a 15−18 times increase in volume after foaming. As shown in Table 1, the maximum foam expansion of PI saturated by pure CO_2 at 5 MPa was

dx.doi.org/10.1021/ie3017658 | Ind. Eng. Chem. Res. 2012, 51, 12827−12834

Table 1. The Expansion Ratio of High-Performance Polymer Foams

polymers	blowing agent	saturation pressure (MPa)	expansion ratio
PEI	CO_2	5	2.5[11]
	CO_2	4.6	2.6[6]
	CO_2	6.5	5.0[16]
	CO_2	5	3.2[a]
PSF	CO_2	5.7	4.8[9]
PESF	CO_2	5.5	3.4[10]
PPSF	CO_2	5.5	4.0[10]
PI	CO_2	5	2.9[a]
	CO_2/THF	5	15.7[a]

[a]The data were obtained from our studies.

about 2.9, which is in the same level with other high-performance polymer foams prepared at a similar foaming condition. This result indicates that the introduction of coblowing agent dramatically increased the foam expansion.

Generally, low gas solubility and high matrix stiffness are thought as important reasons to explain the technological challenges in preparing lightweight high-performance polymer foams.[17] As measured in this study, the solubility of CO_2 in PI matrix was only 4.2 wt % at 5 MPa and 80 °C, while the solubility of THF in PI was 24.0 wt % at the atmospheric pressure and room temperature. It is known that blowing agent can plasticize polymer matrix, and then reduce its T_g as well as matrix stiffness.[18,19] The higher sorption of blowing agent would result in a softer polymer matrix, which facilitated the foam expansion process.[14,20]

Figure 2 show the cell morphology of PI bead foam with three different magnifications. For comparison, the cell morphology of PI foam prepared using CO_2 is also presented. PI foam exhibited a uniform cell structure with cell size of 1.1 μm and cell density of 1.7×10^{12} cells/cm^3. In the case of PI bead foam prepared using the mixed blowing agents, a SEM micrograph with magnification of ×100 (Figure 2b) indicated that PI bead foam possessed tiny cell size and uniform cell structure distribution except at the foam's center. A higher magnification of ×1000 (Figure 2c) showed that PI foams had closed cells, the average cell size was 14.5 μm, and the cell density was 4.2×10^9 cells/cm^3, which demonstrated the successful preparation of a microcellular structure in lightweight PI foams. Compared to the cell morphology of PI foams shown in Figure 2a and 2c, it is indicted that the introduction of THF significantly increased the cell size of PI foams. A SEM micrograph with ×4000 (Figure 2c) suggested that smaller cells with size of 6.8 μm were present in the foam's center, due to the nonequilibrium sorption of the blowing agent.

Organic solvent usually presents higher solubility in polymer than that of the compressed gas.[19] The foamed sample using organic solvent shows extra-low cell density and a high expansion ratio, resulting from low supersaturation and poor cell nucleation according to the classical nucleation theory.[21] On the contrary, the compressed CO_2 induced high cell nucleation and low foam expansion. Our present results demonstrated that the mixed blowing agents facilitated both the cell nucleation process and the foam expansion process, leading to the preparation of lightweight PI foams with microcellular structure.

Preparation of MPI Samples by Compression Molding. Steam-chest molding is a commercial method used to manufacture molded bead foam products and has been widely described in references for the expanded PP bead foam (EPP) fabrication.[22−24] By utilizing the steam-chest molding machine, a 3-dimensional molded bead foam product with a specific shape can be produced. During the steam-chest molding process, high temperature steam is injected periodically into the mold from two directions to soften and fuse the beads. Meanwhile, the steam can penetrate and condense in the cell structure. When the mold is depressurized, the condensed water in the cells begins to gasify and contribute to expansion

Figure 1. Optical micrographs of PI beads and the foamed PI beads. The apparent density of PI bead foam was 82 kg/m^3.

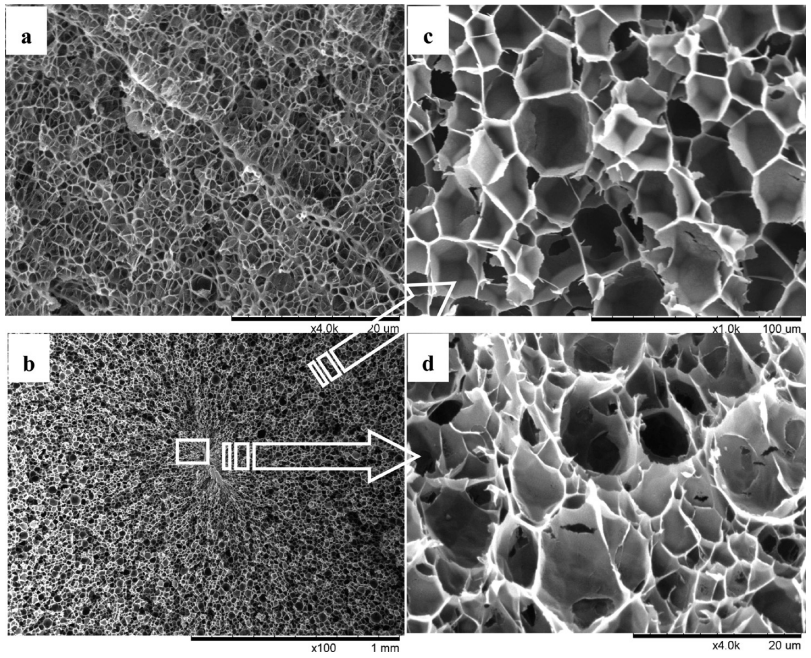

Figure 2. SEM micrographs of PI foams with various magnifications. (a) PI foam was prepared using CO_2, (b) PI foam was prepared using the mixed blowing agents. panels c and d are the locally amplified SEM micrographs of panel b.

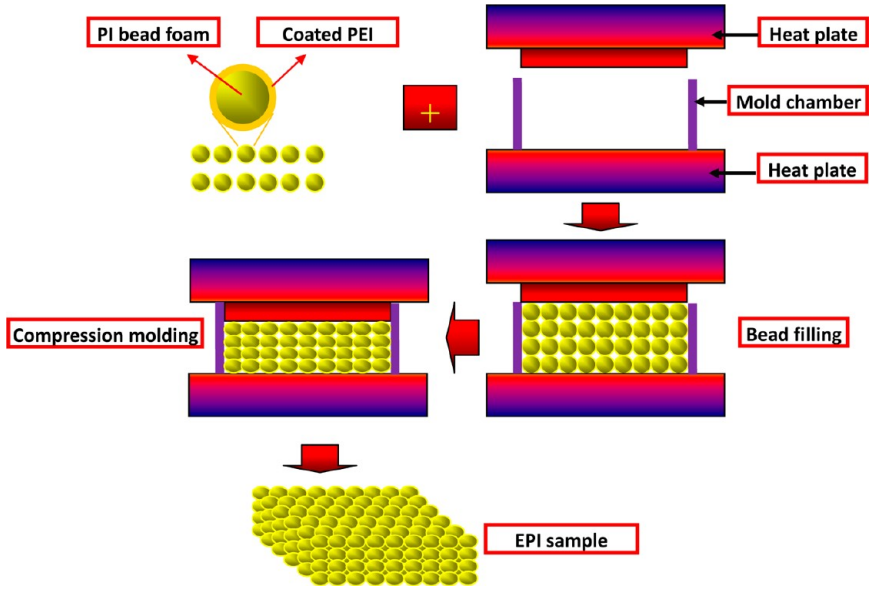

Figure 3. Schematic illustration of the compression molding process of the foamed PI beads.

of the foams together with the expanding air, resulting in the formation of the fused interfaces between the beads. With the help of the water cooling that follows, the fused interfaces solidify and efficient bonding is made between the beads foams.[22]

Our present study suggests that the traditional steam-chest molding process is not suitable for PI bead foam molding. The reason is that the T_g of PI is 265 °C, and the required steam temperature to melt the bead foams' surface is at least 280−320 °C. The generation of steam with such high temperature is difficult and somewhat dangerous. Furthermore, it was found that the foamed PI beads in hot air tended to shrink rather than surface fuse and expand. On the basis of our understanding, therefore, it is impossible to manufacture the foamed PI beads by steam-chest molding.

The formation of soft layers around the PI bead foam is a key issue for PI bead foam molding. To solve this problem, a novel molding mechanism, as indicated in Figure 3, was suggested. It was found that PEI resin was solvable in chloroform, a low boiling point solvent, while the foamed PI beads were not solvable. Therefore, the PEI solution could work as the soft layer of foamed PI beads to generate the interbead bonding. In the suggested molding procedure, the PEI/chloroform solution was coated onto the foamed PI beads' surface. The coated foamed PI beads were transferred into a mold cavity rapidly, and the mold cavity was hot pressed at 200 °C for 1 h to evaporate the solvent. Accompanying with the solvent

Figure 4. Optical micrograph of the molded PI bead foam product.

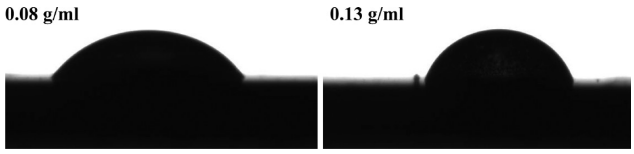

Figure 5. Contact angle between PEI solution (with concentration of 0.08 and 0.13 g/mL) and PI foams.

evaporation, the PEI resin solidified, and the strong bonding was generated between the foamed PI beads. After the compression molding, the prepared MPI product was removed from the mold cavity.

Figure 4 shows the optical micrograph of the obtained MPI product, and the apparent density is 137.7 kg/m^3. It is observed that thousands of PI bead foams stuck together forming a circular plate. Furthermore, the molded sample possessed a dense and shining surface, resulting from the coated PEI layer. It should be pointed out that some voids were still present on the sample's surface and inside the sample, because of the nonexpandable nature of PI foams during the process, even though an extremely high compression force was applied. Filling those voids by PEI solution tended to increase the sample density significantly.

Infiltration Character of PEI Solution on the Surface of the PI Foams. The infiltration nature of PEI solution on PI foam determines the compatibility between the PEI layer and PI foams' surface, which significantly affects the mechanical properties of MPI. The PEI/chloroform solutions with two concentrations of 0.08 and 0.13 g/mL were prepared. Figure 5 shows the contact angles of PEI solutions on PI foam. For PEI solution with a concentration of 0.08 g/mL, the contact angle was 45.8°, which demonstrated that the PEI solution was highly compatible with the PI foam, possibly because of the similar molecular structure between PEI resin and PI resin as well as the good spreading ability of chloroform on PI foam. At a higher PEI solution concentration of 0.13 g/mL, the contact angle increased up to 62°, suggesting a decreased infiltration ability of PEI solution at the increased concentration.

An SEM micrograph was used to further explore the infiltration behavior of PEI solution on the surface of PI bead foam, where MPI samples were broken by bending. Figure 6 panels a, c, and d show the fracture surface of MPI foam with various magnifications, and Figure 6b shows the cell morphology of MPI foam. As indicated in Figure 6a,c, the solidified PEI layer was uniformly coated on the PI bead foam surface, and no obvious PEI layer exfoliation was observed during bending. At higher magnification of ×2000, the PEI layer with thickness of 2.9 μm was observed. It is noted that the fracture mode of MPI foam shown in Figure 6a was almost 100% intrabead fracture. This suggested that the thin PEI layers with a thickness of 2.9 μm were stronger than PI bead foams with a value of 1−3 mm; if not, the crack path tended to run through the bead boundaries. Therefore, the well-defined infiltration character of PEI solution on PI foam's surface potentially endowed MPI foam with strong interbead bonding.

Interbead Bonding of MPI. As suggested in ref 23, the interbead bonding force and the interbead bonding regions per unit volume determine the mechanical properties of the

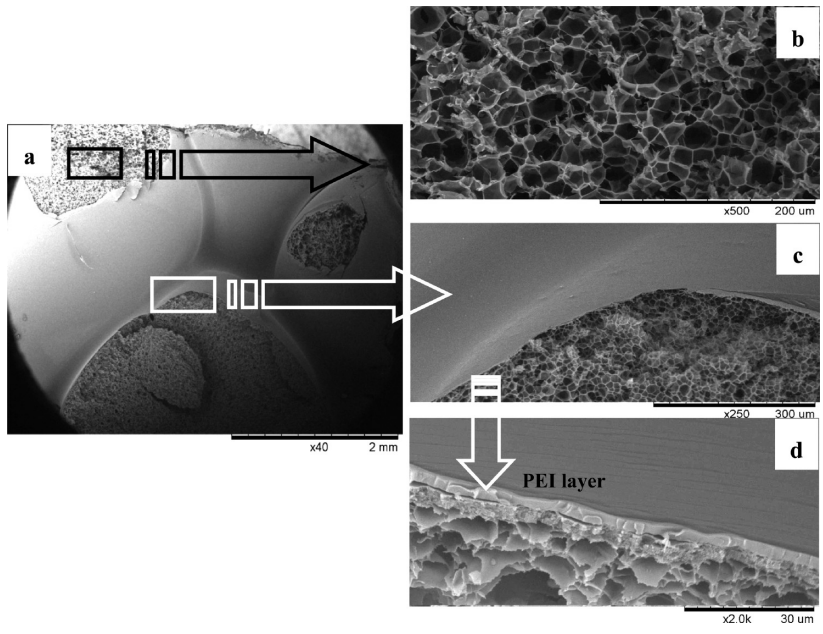

Figure 6. SEM micrographs illustrating the infiltration behavior of PEI solution to the foamed PI beads.

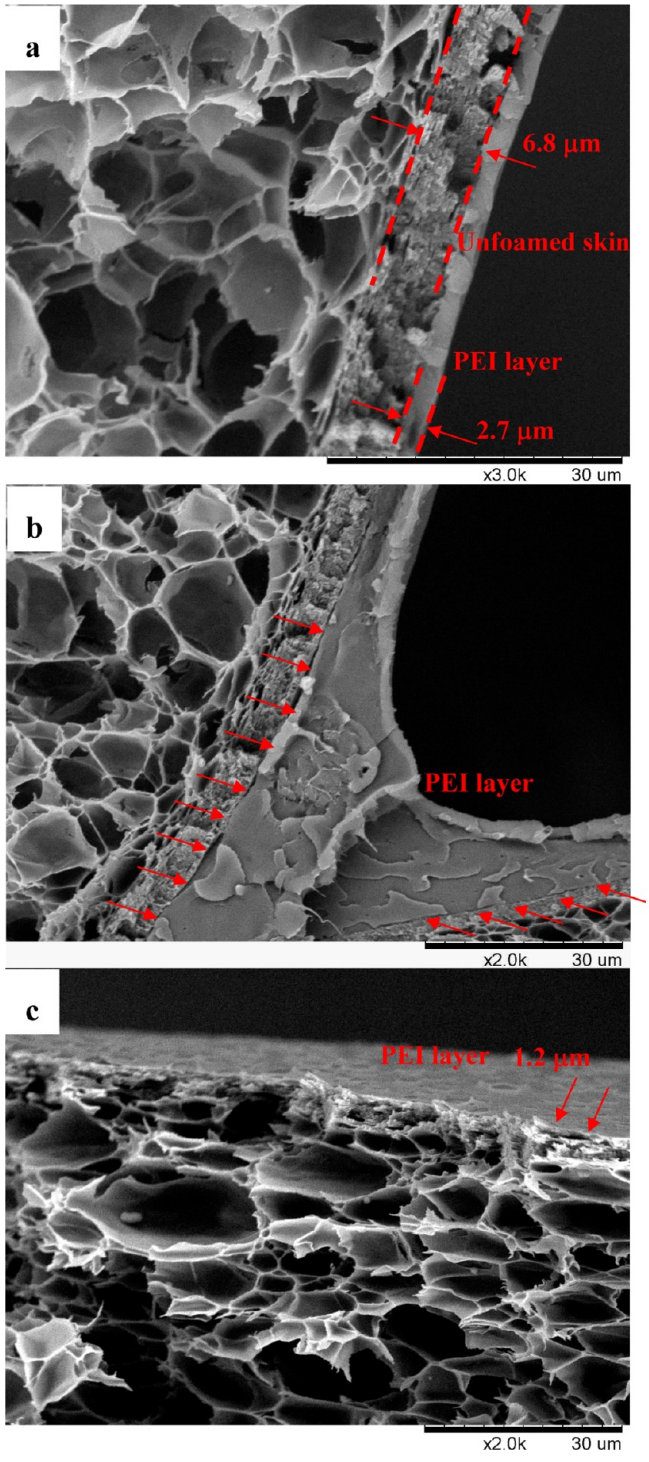

Figure 7. SEM micrographs illustrating the thickness of PEI layer on PI foams. The PEI solution concentrations were 0.13 g/mL (a, b) and 0.08 g/mL (c), respectively.

Table 2. The Bending Strength of MPI Products

	by changing the solution concentrations		by changing the compression force		
	MPI-1	MPI-2	MPI-3	MPI-1	MPI-4
concentration (g/mL)	0.08	0.13	0.08	0.08	0.08
apparent density (kg/m^3)	115.5	121.6	93.7	115.5	137.7
bending strength (MPa)	0.51	1.16	0.34	0.51	1.27

molded foam products. In this study, we investigated their effects on the bending properties of MPI by changing the PEI solution concentration and the applied compression force during the molding.

The interbead bonding force was adjusted by the thickness of PEI layers, where PEI/chloroform solutions with 0.08 and 0.13 g/mL were used and the same compression force was applied. Figure 7 shows the fracture surfaces of MPI after bending. As shown in Figure 7a, PI bead foam had a typical unfoamed skin with a thickness of 6.8 μm, resulting from rapid gas diffusion. Outside the unfoamed skin, a PEI layer with thickness of 2.7 μm was tightly coated on it. For the contact regions of two bead foams, it is observed in Figure 7b that the PEI layer was much thicker than it was at other places. The possible reason is that the PEI solution was forced out of the contact regions of bead foams during compression molding. Figure 7c presented that the thickness of PEI was about 1.2 μm when the applied concentration of PEI solution was 0.08 g/mL. Even thought the PEI layer was much thinner than the diameter of PI bead foam at this situation, that is, 1.2 μm versus 4.0−4.5 mm, the foamed PI beads were broken together with the PEI layer during bending. This phenomenon suggests that the interbead bonding generated by the PEI layer was extremely strong, otherwise, the breaking tended to develop along the interfaces between PI bead foam and PEI layer.

The bending strength of MPI products that were coated by PEI solution with two different concentrations were summarized in Table 2. At PEI solution concentration of 0.08 g/mL, the apparent density of the prepared MPI-1 product was 115.5 kg/m^3, and the bending strength was 0.51 MPa. With the increase in PEI solution concentration to 0.13 g/mL, however, the apparent density of MPI-2 sample increased up to 121.6 K kg/m^3, and the bending strength increased up to 1.16 MPa. These results indicated that an increase in apparent density of 5.3% led to a 125.0% increase in PEI layer thickness, resulting in a 127.5% increase in bending strength.

The interbead bonding region per unit volume was adjusted by applying different compression forces while keeping the PEI solution concentration constant. Figure 8 shows the fracture surfaces of MPI after bending. As seen in Figure 8a, the sample showed interbead fracture behavior, and a huge void was present among the bead foams. Furthermore, the cracks of the MPI sample developed only along interfaces, and the foamed PI beads were not broken during bending. With the increase in compression force, however, the sample exhibited intrabead fracture behavior, and the void area among the bead foam was obviously reduced (Figure 8b). At higher compression force, the void area among bead foams tended to decrease continuously, and the 100% intrabead fracture was observed for the MPI sample.

Table 2 summarizes the bending strength of MPI samples obtained at different compression forces. For the MPI-3 sample with an apparent density of 93.7 kg/m^3, where the lowest compression force was applied, its bending strength was 0.34 MPa. The increase in compression force tended to increase the apparent density of the MPI-1 samples to 115.5 kg/m^3, leading to the increased bending strength of 0.51 MPa. For the MPI-4 sample prepared by the largest compression force, the apparent density was 137.7 kg/m^3, and the bending strength was 1.27 MPa. This suggests that a 19.2% increase in apparent density resulted in a 149.0% increase in bending strength, due to the increased interbead bonding regions.

dx.doi.org/10.1021/ie3017658 | Ind. Eng. Chem. Res. 2012, 51, 12827−12834

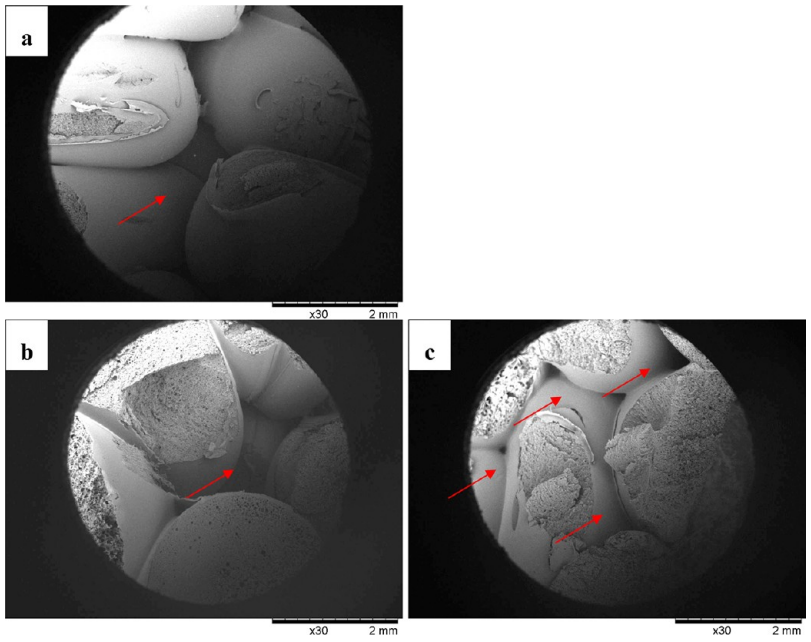

Figure 8. SEM micrographs illustrating the formation of void areas in (a) MPI-3, (b) MPI-1, and (c) MPI-4 samples with the application of various compression forces.

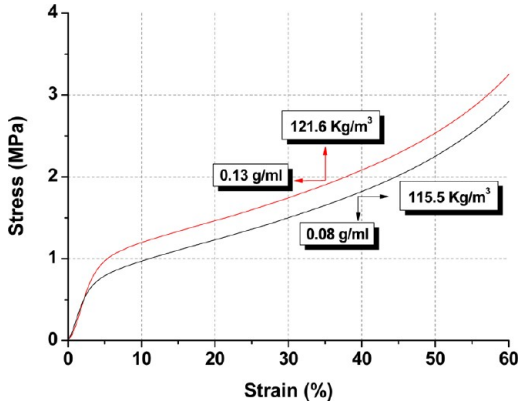

Figure 9. Compressive stress−strain behavior of MPI samples with various PEI solution concentration.

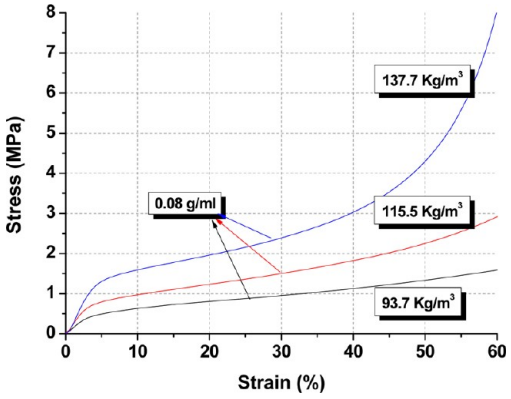

Figure 10. Compressive stress−strain behavior of MPI samples with the application of various compression forces.

In summary, both the thickness of PEI layer and the interbead bonding regions are important parameters to determine the interbead bonding. By adjusting their values, it is possible to adjust the bending properties of MPI product efficiently.

Compression Properties of MPI Products. Compression behaviors are critical properties of PI foams because of their application. Generally, three stages of deformation are commonly observed during compression of polymeric foams.[25] The first stage is characterized by linear elastic response, where stress increases linearly with deformation and the strain is recoverable. The second stage is characterized by continued deformation at relatively constant stress, which provides the bulk of the energy absorption capabilities for the material. The final stage of deformation is densification, where the foam begins to respond as a compacted solid. At this situation, the cellular structure within the foams is collapsed and a further compression induces the deformation of the solid foam material.

Figures 9 and 10 show the compressive stress−strain behavior of MPI products obtained at different conditions. It is seen that the typical linear elastic regions were present in all MPI samples, which occurred with a 5% deformation. With the increase in strain, the gradual increase in stress was observed, and samples with higher density exhibited higher strain dependence. Compared to MPI-1 and MPI-3 samples, however, MPI-4 presented obvious densification at the strain of 50−60%. On the basis of the information supplied by Figure 8, it was believed that MPI-4 possessed less interbead void fraction; the cell structure within the foam started to deform at low strain. Furthermore, the compression stress of MPI-4 at 50% strain was 4.31 MPa, which is much higher than conventional PI structure foams such as TEEK PI foam with a similar density,[26] related to their microcellular structure. In the past study, NASA Langley Research Center investigated the effect of friable balloons on the compression properties of PI foam,[26] where the Nomex core possessed high compressive strength of 2.0 MPa at 50% deflection. They found that the final density of the filled PI foam was 80 kg/m^3, and the addition of honeycomb resulted in a 25% increase for PI foam. Compared with the latter, it seems

dx.doi.org/10.1021/ie3017658 | Ind. Eng. Chem. Res. 2012, 51, 12827−12834

that the prepared MPI foam in this study exhibited better compression properties.

CONCLUSIONS

Microcellular PI foams were prepared using a solid-state foaming process. An organic coblowing agent dramatically increased the gas solubility in PI matrix, which resulted in a significant increase in foam expansion from 2.9 to 15.7. To fabricate the foamed PI beads into the useful 3-D shaped foam product, a novel molding process was suggested in this study, where the PEI/chloroform solution was used as gel and was coated onto the foamed PI beads' surface. The contact angle tests indicated that the PEI solution could spread out on the PI foam surface, and the further SEM observation presented that the PEI layer thickness was about 2.7 μm at a solution concentration of 0.13 g/mL that was tightly stuck outside the foamed PI beads. The solution concentration and the compression force were verified as important parameters to determine the bending and compression properties of MPI foams. By applying a high compression force and a high solution concentration, the prepared MPI foams exhibited an extremely high compression stress of 4.31 MPa at 50% strain. The well-defined mechanical properties potentially endows the lightweight PI foam product with a wide range of applications in aerospace, special ships, and other similar uses.

AUTHOR INFORMATION

Corresponding Author

*Tel.: +86 0574 8668 5256. Fax: +86 0574 8668 5186. E-mail: wtzhai@nimte.ac.cn.

Notes

The authors declare no competing financial interest.

ACKNOWLEDGMENTS

The authors are grateful to Nanjing Yuezi Chemical Ltd, the National Natural Science Foundation of China (Grant 51003115), and the Ningbo Natural Science Foundation (Grant 2011A610118) for their financial support of this study.

REFERENCES

(1) Weiser, E. S.; St Clair, T. L.; Echigo, Y.; Kaneshiro, H.; Grimsley, B. W. Polyimide foams for aerospace vehicles. *High Perform. Polym.* **2000**, *12*, 1−12.

(2) Guo, H.; Meador, M. A. B.; McCorkle, L.; Quade, D. J.; Guo, J.; Hamilton, B.; Cakmak, M.; Sprowl, G. Polyimide aerogels cross-linked through amine functionalized polyoligomeric silsesquioxane. *ACS Appl. Mater. Interfaces* **2011**, *3*, 546−552.

(3) Meador, M. A. B.; Malow, E. J.; Silva, R.; Wright, S.; Quade, D.; Vivod, S. L.; Guo, H.; Guo, J.; Cakmak, M. Mechanically strong, flexible polyimide aerogels cross-linked with aromatic triamine. *ACS Appl. Mater. Interfaces* **2012**, *4*, 536−544.

(4) Pan, L. Y.; Zhan, M. S.; Wang, K. Preparation and characterization of high-temperature resistance polyimide foams. *Polym. Eng. Sci.* **2010**, *50*, 1261−1267.

(5) Krause, B.; Boerrigter, M. E.; van der Vegt, N. F. A.; Strathmann, H.; Wessling, M. Novel open-cellular polysulfone morphologies produced with trace concentrations of solvents as pore opener. *J. Membr. Sci.* **2001**, *187*, 181−192.

(6) Krause, B.; Sijbesma, H. J. P.; Munuklu, P.; van der Vegt, N. F. A.; Wessling, M. Bicontinuous nanoporous polymers by carbon dioxide foaming. *Macromolecules* **2001**, *34*, 8792−8801.

(7) Krause, B.; Diekmann, K.; van der Vegt, N. F. A.; Wessling, M. Open nanoporous morphologies from polymeric blends by carbon dioxide foaming. *Macromolecules* **2002**, *35*, 1738−1745.

(8) Krause, B.; Koops, G. H.; van der Vegt, N. F. A.; Wessling, M.; Wubbenhorst, M.; van Turnhout, J. Ultralow-k dielectrics made by supercritical foaming of thin polymer films. *Adv. Mater.* **2002**, *14*, 1041−1046.

(9) Sun, H. L.; Mark, E. J. Preparation, characterization, and mechanical properties of some microcellular polysulfone foams. *J. Appl. Polym. Sci.* **2002**, *86*, 1692−1701.

(10) Sun, H. L.; Sur, G. S.; Mark, J. E. Microcellular foams from polyethersulfone and polyphenlsulfone: Preparation and mechanical properties. *Eur. Polym. J.* **2002**, *38*, 2373−2381.

(11) Miller, D.; Chatchaisucha, P.; Kumar, V. Microcellular and nanocellular solid-state polyetherimide (PEI) foams using subcritical carbon dioxide I. Processing and structure. *Polymer* **2009**, *50*, 5576−5584.

(12) Miller, D.; Kumar, V. Microcellular and nanocellular solid-state polyetherimide (PEI) foams using subcritical carbon dioxide II. Tensile and impact properties. *Polymer* **2011**, *52*, 2910−2919.

(13) VanHouten, D. J.; Baird, D. G. Generation and characterization of carbon nanofiber−poly(arylene ether sulfone) nanocomposite foams. *Polymer* **2009**, *50*, 1868−1876.

(14) VanHouten, D. J.; Baird, D. G. Generation of low-density high-performance poly(arylene ether sulfone) foams using a benign processing technique. *Polym. Eng. Sci.* **2009**, *49*, 44−51.

(15) Sorrentino, L.; Aurilia, M.; Cafiero, L.; Iannace, S. Nanocomposites foams from high performance thermoplastics. *J. Appl. Polym. Sci.* **2011**, *122*, 3701−3711.

(16) Sorrentino, L.; Aurilia, M.; Iannace, S. Polymeric foams from high-performance thermoplastics. *Adv. Polym. Tech.* **2011**, *30*, 234−243.

(17) Wang, J.; Cheng, X. G.; Yuan, M. J.; He, J. S. An invstigation on the microcellular structure of polystyrene LCP blends prepared by using supercritical carbon dioxide. *Polymer* **2001**, *42*, 8265−8275.

(18) Zhai, W. T.; Yu, J.; Ma, W. M.; He, J. S. Influence of long-chain branching on the crystallization and melting behavior of polycarbonates in supercritical CO_2. *Macromolecules* **2007**, *40*, 73−80.

(19) Zhai, W. T.; Yu, J.; Ma, W. M.; He, J. S. Cosolvent effect of water in supercritical carbon dioxide facilitating induced crystallization of polycarbonate. *Polym. Eng. Sci.* **2007**, *47*, 1338−1343.

(20) Li, B. X.; Yu, J.; Ding, Y. S.; Zhang, J.; He, J. S. Foaming Behavior of Compatible PMMA/$[C_{12}MIM][PF_6]$ System by Supercritical CO_2. *Chem. J. Chin. Univ.*, **2010**, *31*, 861−863.

(21) Colton, J. S.; Suh, N. P. Nucleation of microcellular foams: Theory and practice. *Polym. Eng. Sci.* **1987**, *27*, 500−503.

(22) Zhai, W. T.; Kim, Y. W.; Park, C. B. Steam-chest modling of expanded polypropylene foams. 1. DSC simulation of bead foam processing. *Ind. Eng. Chem. Res.* **2010**, *49*, 9822−9829.

(23) Zhai, W. T.; Kim, Y. W.; Jung, D. W.; Park, C. B. Steam-chest modling of expanded polypropylene foams. 2. Mechanism of interbead bonding. *Ind. Eng. Chem. Res.* **2011**, *50*, 5523−5531.

(24) Nakai, S.; Taki, K.; Tsujimura, I.; Ohshima, M. Numerical simulation of a polypropylene foam bead expansion process. *Polym. Eng. Sci.* **2008**, *48*, 107−115.

(25) Ouellet, S.; Cronin, D.; Worswick, M. Compressive response of polymeric foams under quasi-static medium and high strain rate conditions. *Polym. Test.* **2006**, *25*, 731−743.

(26) Kuwabara, A.; Ozasa, M.; Shimokawa, T.; Watanabe, N.; Nomoto, K. Basic mechanical properties of balloon-type TEEK-L polyimide foam and TEEK-L filled aramid-honeycomb core materials for sandwich structures. *Adv Composite Mater.* **2005**, *14*, 343−363.